

ANALYSIS OF THE CONVERGENT CHANNEL AS AN EXTENSIONAL RHEOMETER

Paulo R. Souza Mendes

pmendes@mec.puc-rio.br

Roney L. Thompson

roney@mec.puc-rio.br

Angela O. Nieckele

nieckele@mec.puc-rio.br

Pontifícia Universidade Católica - Departamento de Engenharia Mecânica
22453-900 - Rio de Janeiro - RJ, Brasil

Abstract. *An important aspect while designing an “ $R^2 z = \text{constant}$ ” convergent channel as an extensional rheometer is the appropriate choice of the geometrical parameters and of the Reynolds number range of operation. The higher is the Reynolds number value, the thinner will be the boundary layer where the undesirable no-slip effect is confined, as discussed in the literature. However, if the Reynolds number, Re , is too large, then shear-related pressure losses become important, which is also undesirable in rheometry. Therefore, one design task is to find a range of Re within which the boundary layer is thin enough, and the velocity field in most of the domain is reasonably close to the desired kinematics. In this work we obtained numerical solutions for the flow of Newtonian and viscoelastic fluids through a convergent channel, for representative ranges of Re , dimensionless channel length, L , and dimensionless axial coordinate of inlet section, z_0 . For all cases, we determined fields of flow type, where regions of shear and of extension can be visualized. Among other findings, it is shown that, depending on the geometrical and flow characteristics, most of the mechanical energy dissipated can be due to shear effects, so that the extensional viscosity cannot be determined via pressure drop measurements.*

Key-words: *Extensional viscosity, Mechanical energy loss*

1. INTRODUCTION

One important feature often observed in flows of viscoelastic liquids through complex geometries is “thinning” in shear-dominated regions and “thickening” in regions of extensional kinematics (James & Walter, 1993). Because these complex flows are often found in practical engineering situations such as fiber spinning, polymer film processing, flows through dies, and many others, an accurate characterization of viscoelastic fluids in extensional flows is of paramount importance.

Perhaps the most exciting present challenge in the field of Rheology is the measurement

of mechanical response of materials under extensional flow. While shear flows are reasonably straightforward to obtain in laboratory, purely extensional flows constitute very difficult — if at all possible— experiments, in particular for mobile polymeric solutions.

One attempt to reproduce uniaxial extensional flows in laboratory is the “constant-extensional-rate channel,” (Shirakashi et al., 1998) which consists of an axisymmetric convergent channel whose wall radial position $R(z)$ obeys the relation $R^2 z = \text{constant}$, where z is the axial coordinate. This geometry is illustrated in Fig. 1.

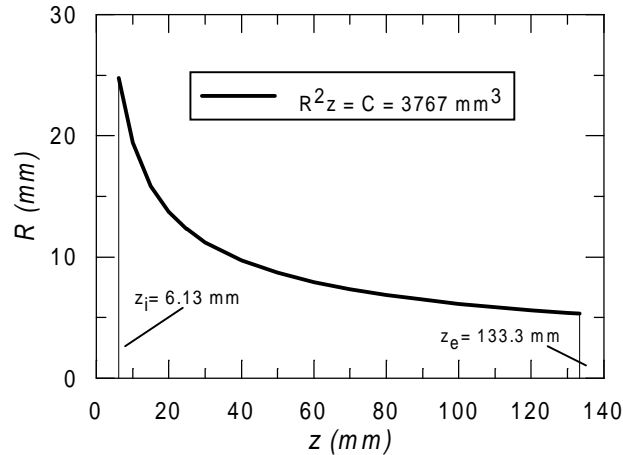


Figure 1. The Convergent Channel

According to James' theory, (James, 1991), the flowing fluid in the core (away from a thin boundary layer at the wall) is subjected to a constant and spatially uniform extension rate. Recent LDV experiments for Reynolds numbers ranging from 100 to 1500 with both Newtonian and elastic liquids (Shirakashi et al., 1998) confirmed that the extension rate is constant along the centerline. However, no information is known regarding the flow field away from the centerline, and the wall effect in the flow field is not assessed.

The goal of the research reported in the present paper is to investigate numerically the flow through the constant-extensional-rate channel. With these numerical solutions it is possible to find the range of Re within which the boundary layer is thin enough, and the velocity field in most of the domain is reasonably close to the desired kinematics.

2. THE ANALYSIS

In this section we present the formulation for the flow through the convergent channel.

2.1 Governing equations

In the present analysis, the liquid is assumed to be incompressible, so that the equation of mass conservation reduces to

$$\text{div } \mathbf{v} = 0 \quad (1)$$

where \mathbf{v} is the velocity vector field.

The momentum equation is, for steady flow and negligible external forces,

$$\rho \text{ div } (\mathbf{v} \mathbf{v}) = - \text{grad } p + \text{div } \boldsymbol{\tau} \quad (2)$$

where p is the pressure, $\boldsymbol{\tau} \equiv \mathbf{T} + p \mathbf{1}$ the extra-stress, \mathbf{T} the stress tensor, and ρ the mass density.

For a Newtonian liquid, $\boldsymbol{\tau} = 2 \mu \mathbf{D}$ where μ is the viscosity, and $\mathbf{D} \equiv [\nabla \mathbf{v} + (\nabla \mathbf{v})^T] / 2$ the rate-of-strain tensor. The non-Newtonian fluid of interest for the present work is a polymeric liquid, which is here represented by the constitutive equation proposed by Thompson et al. (1999). The features of this equation which are needed in the present work are briefly described next.

2.2 Flow classification

The relative-rate-of-rotation tensor (Drouot and Lucius, 1976), $\overline{\mathbf{W}}$, is a key kinematic quantity in flow classification. It is defined as

$$\overline{\mathbf{W}} = \mathbf{W} - \boldsymbol{\Omega} \quad (3)$$

where \mathbf{W} vorticity tensor, defined as $[\nabla \mathbf{v} - (\nabla \mathbf{v})^T] / 2$.

The quantity $\boldsymbol{\Omega}$ is a tensor related to the rate of rotation of \mathbf{D} following the motion. If the set of unit vectors $\{\mathbf{e}_i^*\}$ is the basis consisting of the principal directions of \mathbf{D} (i.e., the eigenvectors of \mathbf{D}) then the vector angular velocity of this basis is defined by

$$\frac{d \mathbf{e}_i^*}{d t} = \mathbf{w} \times \mathbf{e}_i^* , \quad i = 1, 2, \text{ or } 3 \quad (4)$$

where d/dt denotes the material time derivative. The angular velocity \mathbf{w} can be represented in the following tensorial form, $\boldsymbol{\Omega}$

$$\boldsymbol{\Omega} \equiv \mathbf{w} \bullet \boldsymbol{\varepsilon} , \quad i = 1, 2, \text{ or } 3 \quad (5)$$

where $\boldsymbol{\varepsilon}$ is the third-rank alternator tensor.

Because $\overline{\mathbf{W}}$ is a difference between two angular velocities, it is clear that it is a frame-indifferent quantity (Astarita, 1979). Astarita (1979) also showed that the ratio

$$R_D \equiv - \frac{\text{tr } \overline{\mathbf{W}}^2}{\text{tr } \mathbf{D}^2} . \quad (6)$$

is a measure of the degree to which the flowing fluid avoids stretching, and can be used to classify flows. R_D has the interesting property of taking the values of 0 in pure extension and 1 in shear flows. Moreover, as the motion approaches a rigid-body motion (i.e., as $\mathbf{D} \rightarrow \mathbf{0}$), it approaches infinity. It is worth noting, however, that $\boldsymbol{\Omega}$ is not defined for rigid-body motion, because $\mathbf{D} = \mathbf{0}$ and hence any direction is a principal direction of \mathbf{D} .

2.3 Constitutive equation

The non-Newtonian fluid is essentially a generalized Newtonian fluid, i. e., $\boldsymbol{\tau} = 2 \eta \mathbf{D}$ where η is the viscosity function, given by (Thompson et al., 1999)

$$\eta(\dot{\gamma}, R_D) = \eta_s(\dot{\gamma})^{R_D} \eta_e(\dot{\gamma})^{1-R_D} \quad (7)$$

where η_e and η_s are related with the deformation rate $\dot{\gamma} \equiv \sqrt{2 \operatorname{tr} \mathbf{D}^2}$ by

$$\eta_e = \eta_o \left[1 + (\lambda \dot{\gamma})^2 \right]^{\frac{n_e-1}{2}} \quad (8)$$

$$\eta_s = \eta_o \left[1 + (\lambda \dot{\gamma})^2 \right]^{\frac{n_s-1}{2}} \quad (9)$$

The viscosity η_e is related with the extensional viscosity by $\eta_e \equiv \eta_E / 3$. Note that, according to equation (7), $\eta \rightarrow \eta_e$ as $R_D \rightarrow 0$ (extensional flow), and $\eta \rightarrow \eta_s$ as $R_D \rightarrow 1$ (shear flow). Therefore, if the parameters of equations (8) and (9) are determined via least-squares fits to experimental data, then the constitutive equation should represent well the material behavior for shear and extensional flows.

2.4 Mechanical energy loss

The uniaxial extensional flow is given by

$$\mathbf{v} = \dot{\epsilon} \left(x_1 \mathbf{e}_1 - \frac{1}{2} x_2 \mathbf{e}_2 - \frac{1}{2} x_3 \mathbf{e}_3 \right) \quad (10)$$

where $\dot{\epsilon}$ is a constant (the extension rate), and \mathbf{e}_i, x_i the unit vector and coordinate in the i -direction, $i=1, 2, 3$.

The rate-of-strain tensor for this flow is simply

$$\mathbf{D} = \dot{\epsilon} \left[\mathbf{e}_1 \mathbf{e}_1 - \frac{1}{2} (\mathbf{e}_2 \mathbf{e}_2 + \mathbf{e}_3 \mathbf{e}_3) \right] \quad (11)$$

therefore, \mathbf{D} does not depend on position.

Knowing that the extensional viscosity η_E is given by

$$\eta_E \equiv \frac{T_{11} - T_{22}}{\dot{\epsilon}} \quad (12)$$

it can be shown that, for an ideal extensional flow,

$$\operatorname{tr}(\boldsymbol{\tau} \bullet \operatorname{grad} \mathbf{v}) = \eta_E \dot{\epsilon}^2 \quad (13)$$

thus, the mechanical energy loss for this ideal flow is

$$\int_{\mathcal{V}} \operatorname{tr}(\boldsymbol{\tau} \bullet \operatorname{grad} \mathbf{v}) \, d\mathcal{V} = \eta_E \dot{\epsilon}^2 \mathcal{V} \quad (14)$$

Figure 2 illustrates a convergent channel $R^2 \, z = C$, where $z \equiv x_1$ is the axial coordinate. The volume of the channel delimited by stations z_1 and z_2 can be easily calculated,

resulting in the following expression for the mechanical energy loss for an ideal extensional flow

$$\int_{\mathcal{V}} \text{tr} (\boldsymbol{\tau} \cdot \text{grad } \mathbf{v})_{\text{ideal}} d\mathcal{V} = \pi C \ln\left(\frac{z_2}{z_1}\right) \eta_E \dot{\epsilon}^2 \quad (15)$$

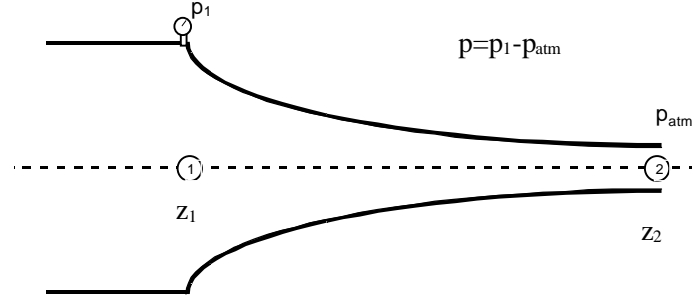


Figure 2 - Pressure taps at a convergent channel

In accordance with Figure 2, the mechanical energy loss is also given by

$$\dot{m} \left[\left(\frac{p}{\rho} + \frac{\bar{v}^2}{2} \right)_1 - \left(\frac{p}{\rho} + \frac{\bar{v}^2}{2} \right)_2 \right] \quad (16)$$

or

$$= Q \Delta p - \frac{\dot{m}}{2} (\bar{v}_2^2 - \bar{v}_1^2) \quad (17)$$

where Q is the volumetric flow rate, which can be calculated for the flow of equation (10) resulting in

$$Q = \dot{\epsilon} \pi C \quad (18)$$

Combining equations (15), (17) and (18), we can write for the ideal extensional flow

$$\eta_E = \frac{\Delta p_E - \frac{\rho \dot{\epsilon}^2}{2} (z_2^2 - z_1^2)}{\dot{\epsilon} \ln \frac{z_2}{z_1}} \quad (19)$$

where Δp_E is the pressure drop for an ideal extensional flow.

However, close to the wall, due to the no-slip condition, the flow is far from being extensional. Moreover, mechanical energy is also dissipated within the boundary layer, and hence the pressure field must be affected. Therefore, it is clear that, in principle, for real flows, the pressure field Δp is larger than Δp_E , due to undesirable shear losses, especially as Re is increased. We wish to know how large, to be able to estimate errors. To quantify this, we employ the ratio

$$E \equiv \int_{\forall} \frac{\text{tr} (\boldsymbol{\tau} \bullet \text{grad } \mathbf{v})_{\text{real}}}{\text{tr} (\boldsymbol{\tau} \bullet \text{grad } \mathbf{v})_{\text{ideal}}} d\forall \quad (20)$$

where the numerator is evaluated by using the numerical results.

3. NUMERICAL METHOD

The conservation equations are discretized with the aid of the finite volume method described in Patankar (1980), using the *power-law* scheme. A non-orthogonal curvilinear system of coordinates, which adapts to the boundaries of the domain, was employed. Staggered velocity components were used to avoid unrealistic pressure fields, and the contra-variant velocity component was selected as the dependent variable in the momentum conservation equations (Pires, 1995 and Pires and Nieckele, 1994). The pressure-velocity coupling was solved by an algorithm based on SIMPLEC (van Doormaal and Raithby, 1984). The resulting algebraic system was solved via the TDMA line-by-line algorithm (Patankar, 1980) with the block correction algorithm (Settari and Aziz, 1973) to increase the convergence rate.

A transfinite interpolation scheme was employed to generate a mesh with 80×40 control volumes. Extensive mesh tests were performed in order to assure essentially mesh-independent results.

4. RESULTS AND DISCUSSION

Numerical solutions were obtained for both Newtonian and non-Newtonian fluid. For the Newtonian fluid, the viscosity was specified as

$$\mu = 100 \text{ Pa}\cdot\text{s} \quad (21)$$

Since the extensional viscosity increases with the deformation rate while the shear viscosity decreases, for typical polymeric liquids, the following parameters were specified

$$\eta_o = 100 \text{ Pa}\cdot\text{s} \quad ; \quad \lambda = 2.656 \times 10^{-3} \text{ s} \quad (22)$$

$$n_e = 1.5 \quad ; \quad n_s = 0.5$$

The results are presented in the form of streamlines, R_D -fields and deformation rate fields. Figures 3 and 4 illustrate the streamlines for $Re = 0.020$ and $Re = 200$ for Newtonian and non-Newtonian fluid, respectively. The flow field is similar for both fluids. It can be observed a thinner boundary layer for the larger Reynolds numbers.

The R_D field is presented on Figures 5 and 6 for both types of fluids. The darkest color corresponds to smallest R_D , indicating the presence of extensional flow. The region where R_D is close to 1, light color, there is shear flow. It can be seen that for low Reynolds number, for both fluids, there is shear flow in almost the entire channel, with the exception of the entrance region. Near the entrance, it can be seen a region of rigid body flow, $R_D \rightarrow \infty$ (the dark region surrounded by the light color). For both fluids, however, this region tends to vanish as Re

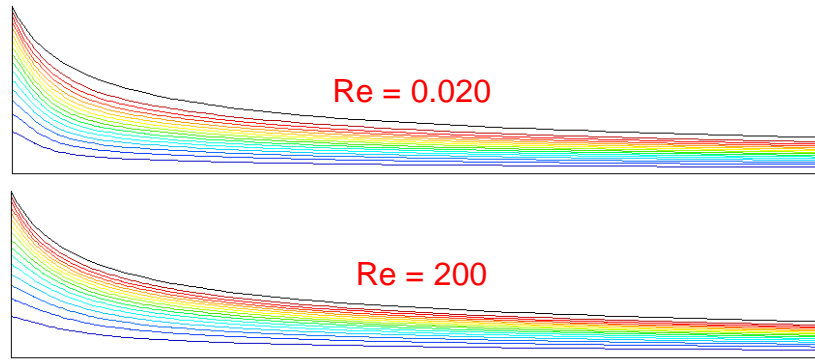


Figure 3 - Streamlines for Newtonian Fluid

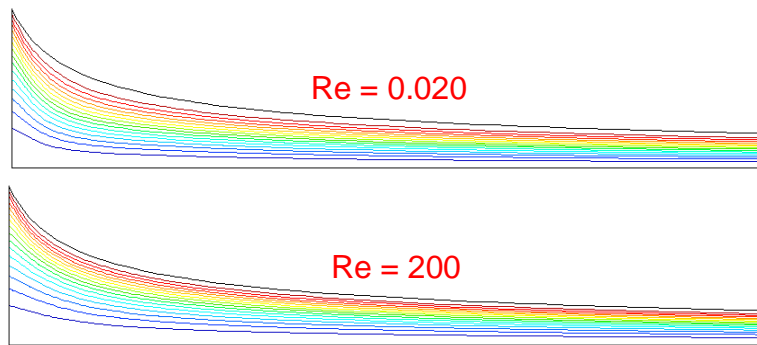


Figure 4 - Streamlines for non-Newtonian Fluid

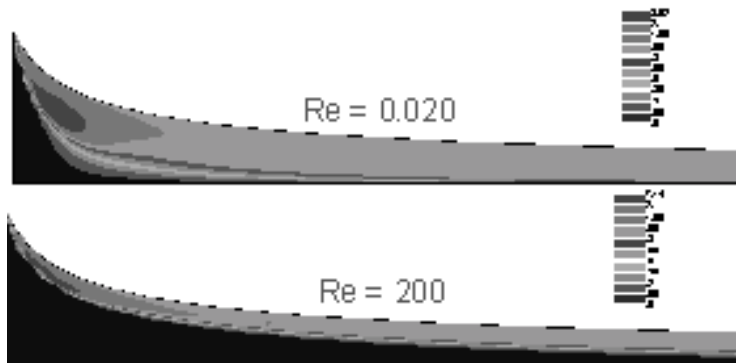


Figure 5 - R_D field for Newtonian fluid

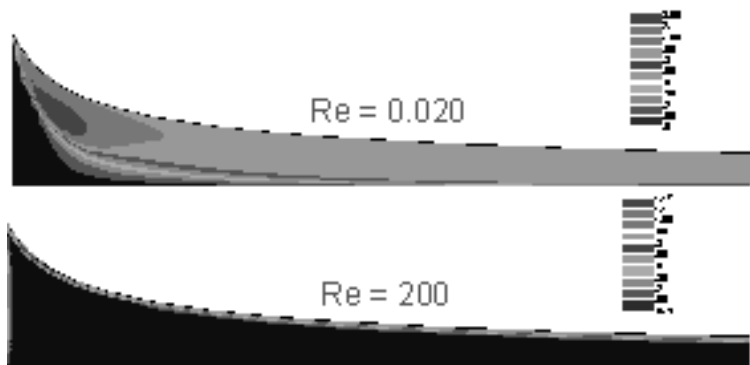


Figure 6 - R_D field for Newtonian fluid

increases. For high Re and non-Newtonian fluid the flow is extensional in almost the entire channel, while the shear flow is limited to a very narrow region. Further, at the near wall region, where the shear flow is present, since the deformation rate is high, the resulting shear viscosity is small, and therefore the approximation of uniaxial extensional flow is better.

The deformation rate fields for the Newtonian and non-Newtonian fluids are illustrated in Figures 7 and 8, respectively, for both Reynolds numbers. Comparing Figures 7 and 8, for $Re = 0.020$, it can be seen that the deformation field is very similar for both fluids, with the same order of magnitude. Near the entrance the deformation rate is low ($\dot{\gamma} < 30$), especially at the solid body motion region, where the deformation rate is negligible. For both fluids, the maximum deformation rate is approximately 700, near the solid surface. For high Reynolds number, the deformation rate is significantly higher ($\approx 1 \times 10^6$) than for low Re , and the high deformation region is confined to the region close to the wall. This behavior is accentuated for the non-Newtonian fluid.

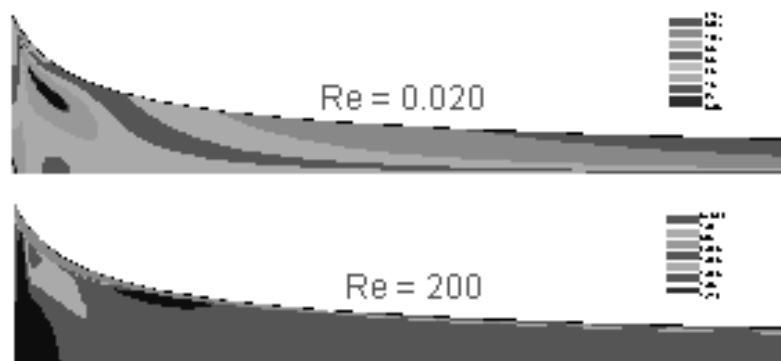


Figure 7 - Deformation rate

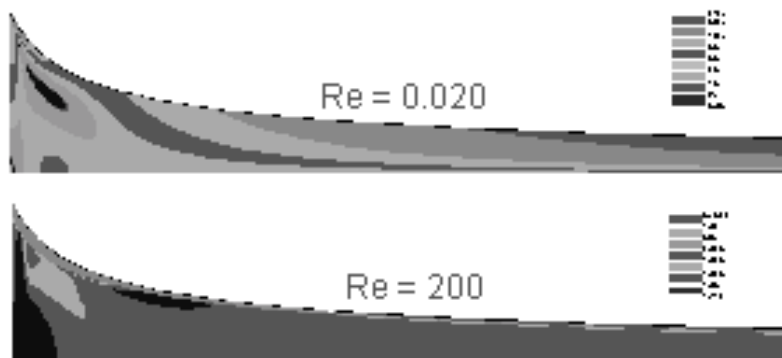


Figure 8 - Deformation rate field for non-Newtonian fluid

The mechanical energy loss relative to ideal extensional flow, E , is shown in Figure 9 for both fluids. For an ideal flow E should be 1. It can be seen that for both liquids, the results obtained are far from the ideal one. For the Newtonian liquid, the relative energy loss is almost constant with the extension rate. This means that the mechanical energy loss in the convergent channel is approximately proportional to the extension rate squared, except for very high extension rates. For low Re and for the non-Newtonian fluid, the relative energy loss is high and analogous to the Newtonian fluid. This result was expected, since not only the R_D field but also the deformation fields are similar. As the extension rate increases (Re also increases), the relative mechanical energy loss reduces significantly, and a better

representation of an ideal extensional flow is obtained. This happens because the flow is extensional in almost the entire domain (low R_D). Near the wall, shear dominates, and although this region also presents high deformation rates, its contribution for the energy loss is small, because the region is very small.

The results show that in the core and away from the inlet and outlet boundaries the flow type is very close to the one desired, namely, the uniaxial extensional flow. However, some important deviations from the desired kinematics are observed.

- For low Re , the wall effect is present throughout;
- For high Re , the wall effect is confined to a boundary layer of roughly uniform thickness. This thickness, however, is rather large for Newtonian fluids, so that much of the flow is not extensional. For non-Newtonian fluids, the shear region is much smaller.
- In the core where extension prevails, the extension rate is quite uniform, as observed experimentally by Shirakashi et al. (1998);
- The rate of shear inside the boundary layer is about two orders of magnitude larger than the rate of extension at the centerline;
- The dissipation of mechanical energy is dominated by shear;
- A region of very low deformation rates appears close to the entrance section, to accommodate the transition between the imposed extensional flow at the inlet and the actual flow, which is affected by the no-slip condition at the wall.

The influence on numerical results of the inflow and outflow boundary conditions is quite clear, indicating that measurements of velocity and stress fields to obtain the extensional viscosity are to be made away from these boundaries. Numerical studies should also be performed to assess the effect of different boundary conditions on the flow.

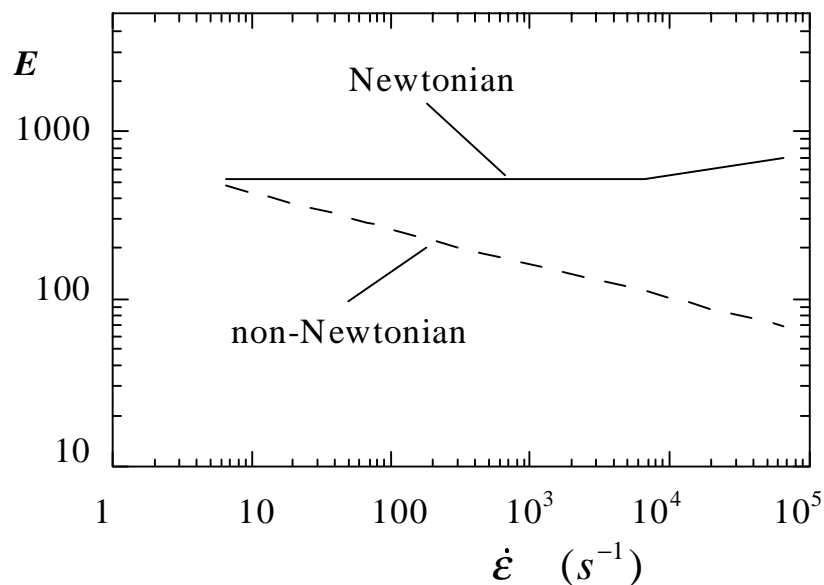


Figure 9 - Mechanical energy loss

5. CONCLUSIONS

A simple analysis of a “ $R^2 z = constant$ ” convergent channel relates the extensional viscosity to measurable quantities.

The numerical results presented show that James' boundary layer theory works well. The analysis showed that for low Re , the flow kinematics are shear dominated and, for shear-thinning, extensional –thickening fluids and high Re , the boundary layer is quite thin.

For Newtonian fluids, mechanical energy losses due to shear can be orders of magnitude higher than the ones related to extension. For shear thinning, extensional–thickening fluids, the situation tends to improve.

As the extensional rate is increased, the performance gets worse for Newtonian fluids and better for shear thinning, extensional-thickening fluids.

It is also seen that shear is present in a region larger than the one assumed in the theory proposed by James (1991). These results also suggest that both the inlet and outlet boundary conditions have an important influence on the flow type inside the channel.

Acknowledgments

This research program has been executed with financial support of CNPq and FAPERJ.

REFERENCES

- Astarita, G., 1979, "Objective And Generally Applicable Criteria For Flow Classification", *J. Non-Newtonian Fluid Mechanics*, vol. 6, pp. 69-76.
- Drouot, R. & Lucius, M., 1976, Approximation Du Second Ordre De La Loi De Comportement Des Fluides Simples. Lois Classiques D'Eduites De L'introduction D'un Nouveau Tenseur Objectif, *Archiwum Mechaniki Stosowanej*, vol. 28, n. 3, pp. 189-198.
- James, D. F., 1991, Flow In A Convergent Channel At Moderate Reynolds Number, *AIChE J.*, vol 37, n. 1, pp. 59-64.
- James, D. F. and Walters, K., 1993, A Critical Appraisal Of Available Methods For The Measurement Of Extensional Properties On Mobile Systems, *Techniques in Rheological Measurement*, Collyer A. A., ed.; Chapman & Hall, Cambridge, pp. 33-53.
- Patankar, S. V., 1980, *Numerical Heat Transfer and Fluid Flow* (Hemisphere Publishing Corporation).
- Pires, L. F. G., 1995, A Numerical Method For The Solution Of Flows Using Contravariant Components In Non-Orthogonal Coordinates, PhD Thesis, Pontifícia Universidade Católica-RJ (in Portuguese).
- Pires, L. F. G. and Niecele, A. O., 1994, Numerical Method For The Solution Of Flows Using Contravariant Components In Non-Orthogonal Coordinates, *Proc. V Brazilian Meeting on Thermal Sciences, SP*, pp. 343-346 (in Portuguese).
- Settari, A. and Aziz, K., 1973, A Generalization of the Additive Correction Methods for the Iterative Solution of Matrix Equations, *SIAM J. Num. Anal.*, vol. 10, pp. 506-521.
- Shirakashi, M., Ito, H. and James, D. F., 1998, LDV Measurement of the Flow Field in a Constant-Extension-Rate Channel, *J. Non-Newtonian Fluid Mechanics*, vol. 74, pp. 247-262.
- Smith, G. F., 1971, On Isotropic Functions Of Symmetric Tensors, Skew-Symmetric Tensors And Vectors, *Int. J. Engng Sci.* vol. 9, pp. 899-916.
- Thompson, R. L., Souza Mendes, P. R., Naccache, M. F., 1999, A New Constitutive Equation and Its Performance in Contraction Flows, *Journal of Non-Newtonian Fluid Mechanics*, (in print)..
- Van Doormaal, J. P. and Raithby, G. D., 1984, Enhancements of the SIMPLE Method for Prediction Incompressible Fluid Flows, *Num. Heat Transfer*, vol. 7, pp. 147-163.